Pharmacological Reports 67 (2015) 245–252

Contents lists available at ScienceDirect

Pharmacological Reports

journal homepage: www.elsevier.com/locate/pharep

Original research article

Antineoplastic effects of deoxypodophyllotoxin, a potent cytotoxic agent of plant origin, on glioblastoma U-87 MG and SF126 cells

Mounia Guerram [a], Zhen-Zhou Jiang [a,b,*], Lixin Sun [a,c], Xiong Zhu [d], Lu-Yong Zhang [a,e,*]

[a] Jiangsu Center for Drug Screening, China Pharmaceutical University, Nanjing, China
[b] Jiangsu Center for Pharmacodynamics Research and Evaluation, China Pharmaceutical University, Nanjing, China
[c] Key Laboratory of Drug Quality Control and Pharmacovigilance (China Pharmaceutical University), Ministry of Education, Nanjing, China
[d] State Key Laboratory of Natural Medicines, China Pharmaceutical University, Nanjing, China
[e] Medical and Chemical Institute, China Pharmaceutical University, Nanjing, China

ARTICLE INFO

Article history:
Received 3 June 2014
Received in revised form 1 October 2014
Accepted 3 October 2014
Available online 19 October 2014

Keywords:
Deoxypodophyllotoxin
Glioblastoma
Cdc2/Cyclin B1

ABSTRACT

Background: Deoxypodophyllotoxin (DPT) is a semi-synthetic compound derived from the extract of *Dysosma versipellis* (Hance) M. Cheng, one of the most popular Chinese herbal medicines. The present study evaluates the *in vitro* cytotoxicity of DPT on a wide panel of human cancer cell lines and investigates its molecular mechanism of action on high grade glioma U-87 MG and SF126 cells.
Methods: The growth inhibitory effect of DPT on different types of human cancer cells was measured by the Cell Counting Kit-8 (CCK-8) assay. For the elucidation of the nature of the cellular response to DPT-treatment; flow cytometry-based assays, light and fluorescent microscopy, caspase colorimetric and inhibition assays, and Western blot analysis were performed.
Results: Our data show that DPT possesses a potent growth-inhibitory action, with IC_{50} values in nanomolar ranges. Cell cycle analysis revealed G2/M phase arrest in a dose- and time-dependent manner before cell death occurred. Additional studies indicated that DPT induced G2 arrest in U-87 MG cells by decreasing the expression of Cdc2, cyclin B1, and Cdc25C proteins. In contrast, DPT failed to down-regulate these cell cycle regulatory molecules in SF126 glioblastoma cells and stopped the cell cycle at M phase. Interestingly, morphological changes and biochemical markers such as phosphatydylserine externalization, DNA fragmentation, and caspase activation, confirmed that DPT-treatment resulted in an induction of apoptosis in both examined cell lines *via* caspase-dependent pathways.
Conclusions: Taken together, our data demonstrated that DPT possesses a potent *in vitro* cytotoxic activity and exerts its effect *via* G2/M arrest and apoptosis.
© 2014 Institute of Pharmacology, Polish Academy of Sciences. Published by Elsevier Urban & Partner Sp. z o.o. All rights reserved.

Introduction

Cancer is a leading cause of human deaths worldwide because of its high incidence and mortality rates. Of all cancer types, glioblastoma multiforme (GBM), the most common malignant primary brain tumor [1], represents the most aggressive and difficult-to-treat cancer in the world accounting for approximately 12–15% of all intracranial neoplasms [2]. The overall annual incidence of GBM is 3.1/100,000 persons [3]. Although enormous advances in treating other cancers have been made [4], only modest advancements in the treatment of GBM have occurred in the past 25 years with a median survival time of approximately 12 months [5].

Deoxypodophyllotoxin (DPT), a semi-synthetic compound derived from the extract of *Dysosma versipellis* (Hance) M. Cheng, is an interesting compound correlated to podophyllotoxin (Fig. 1A), a cyclolignan with important antineoplastic and antiviral properties [6]. *D. versipellis* is one of the most popular Chinese herbal medicines. It is a rare and vulnerable perennial herb [7] belonging to Berberidaceae [8] mainly growing in areas of Zhejiang, Jiangxi and Hubei [9]. In traditional Chinese medicine, the plant's rhizome and roots have long been used to treat cough, tuberculosis, parotitis, fracture, rheumatoid arthritis, lumbago, skelalgia, and

* Corresponding authors.
E-mail addresses: beaglejiang@cpu.edu.cn (Z.-Z. Jiang), lyzhang@cpu.edu.cn (L.-Y. Zhang).

http://dx.doi.org/10.1016/j.pharep.2014.10.003
1734-1140/© 2014 Institute of Pharmacology, Polish Academy of Sciences. Published by Elsevier Urban & Partner Sp. z o.o. All rights reserved.

snake bites [10,11]. Previous studies have indicated that constituents and extracts of this traditional Chinese medicinal plant possess potent growth inhibitory properties against different types of tumors [12–14]. In recent decades, *D. versipoellis* has attracted the interest of the pharmaceutical industry due to the presence of podophyllotoxin, an aryltetralin lignan used as the starting material for the preparation of the well-known cytostatic agents: etoposide and teniposide [6,15–17] which are used in combination therapies with other drugs for the treatment of a variety of malignancies.

Although there has been some research on DPT, its antitumor activity as well as the specific mechanism by which it exerts its cytotoxic effect against high grade glioma cells, have not been investigated before. The present study aimed to evaluate the *in vitro* antiproliferative activity of DPT against various human cancer cell lines and to investigate its molecular mechanism of action on glioblastoma-derived U-87 MG and SF126 cells. The concentration and time dependence of the DPT effect was also examined.

Materials and methods

Drugs

DPT (MW 398 g/mol) was provided by China Pharmaceutical University Research Institute of Pharmaceutical Chemistry. It was obtained as a white powder of high purity (>98%). A 10^{-2} M stock solution of DPT was prepared in dimethyl sulfoxide (DMSO, Sigma). Etoposide was purchased from the National Institute for Food and Drug Control (NIFDC, China). Paclitaxel (30 mg/5 ml) was purchased from Shenzhen Main Luck Pharmaceuticals Inc. (China). All drugs were diluted in serum-free media.

Cells and culture conditions

Human glioblastoma-astrocytoma, epithelial-like cell line U-87 MG and gastric carcinoma SGC-7901 cells were maintained in DMEM medium. The culture medium for human glioblastoma SF126 cells was MEM medium. BGC-823 (gastric carcinoma), HO-8910 (ovarian carcinoma), and JeG-3 (human choriocarcinoma) cells were grown in RPMI 1640. Human ovarian cancer SK-0V-3 cell line was maintained in McCoy'5A medium. Human colon carcinoma HT-29 cells were maintained in DMEM/F12 (1:1) medium. The culture medium for MDA-MB-231 cells (breast carcinoma) was Leibovitz's L-15 medium. Media were supplemented with 10% (v/v) fetal bovine serum.

Except U-87 MG cells which were procured from American Type Culture Collection (ATCC, Rockville, MD); all other cell lines were obtained from the Cell Bank of Shanghai Institute of Cell Biology, Chinese Academy of Sciences (Shanghai, China).

In vitro *cytotoxicity screening*

The chemosensitivity of the different tumor cell lines to DPT and etoposide was evaluated *in vitro* with a Cell Counting Kit-8 (CCK-8) test. In brief, cells in logarithmic growth phase were plated at a density of 2000–10,000 cells per well in 96 well plates. After 24 h in culture, cells were exposed to various concentrations of the test drugs (three wells per concentration) for 72 h. At the end of the incubation period, cell proliferation was assessed using the CCK-8 assay. The absorbance intensity of each well was measured at 450 nm with Bio-Rad 680 microplate reader (Bio-Rad Laboratories, Hercules, CA, USA).

The inhibitory rate of cell proliferation was calculated as: $(OD_{control} - OD_{treated\ sample})/OD_{control} \times 100$. The 50% inhibitory concentrations (IC_{50}) were calculated using the dose–response fitted curves (Origin Labs OriginPro v8.0).

Cell cycle analysis

The antitumor action of DPT was studied on brain tumor U-87 MG and SF126 cell lines. After DPT-treatment, cells were harvested, washed with phosphate buffered saline (PBS) and fixed in ice-cold 70% (v/v) ethanol at 4 °C overnight. The fixed cells were then centrifuged at $1000 \times g$ for 5 min, washed with PBS and resuspended in staining buffer containing RNase and propidium iodide (PI). After incubation for 30 min in the dark, cell cycle distribution was determined by flow cytometry. Data were acquired using CellQuest software and cell cycle analysis was performed using ModFit LT software.

Morphological analysis of DPT-treated cells by light microscopy

U-87 MG and SF126 cells were grown in 60-mm culture dishes under standard culture conditions. After 24 h in culture, cells were treated with DPT (90 nM) and incubated for lengths of time ranging from 12 to 36 h. Control cells without DPT-treatment were incubated under identical conditions. Morphological changes were observed by phase contrast microscopy (Olympus IX71, Tokyo, Japan).

Immunocytochemistry

Cells attached to coverslips were either untreated or treated with DPT for 12 and 36 h. After treatment, cells were fixed with 4% paraformaldehyde, permeabilized in 0.1% Triton X-100 and washed with phosphate buffered saline Tween 20 (PBST). Non-specific sites were then blocked by 2% bovine serum albumin (BSA). A mouse monoclonal antibody against α-tubulin was incubated with cells for 1 h at room temperature. Cells were then washed with PBST to remove excess antibody and then probed with Alexa-Fluor 488-conjugated secondary antibody. Nuclear DNA was stained with Hoechst 33258 dye (Invitrogen, CA, USA). The images were captured with an Olympus IX71 fluorescence microscope (Tokyo, Japan).

Annexin-V/PI binding assay

Flow cytometric analysis with Annexin V-FITC Apoptosis Detection Kit I (BD Biosciences Pharmingen, San Diego, CA) was performed according to the manufacturer's instructions to evaluate Annexin-V/PI positivity. Cells were sorted by flow cytometry using a FACS flow cytometer (Becton Dickinson, San Jose, CA, USA).

Determination of caspase activity

The activity of caspase-3, -8, and -9 was determined using Caspase Activity Assay Kits following the protocol of the manufacturer. Briefly, glioblastoma cells treated with or without DPT were collected, lysed in a lysis buffer and clarified by centrifugation. After protein quantification by the Bradford assay; cell lysates were mixed with the assay buffer and 10 μl of the substrate: Ac-DEVD-pNA (caspase-3), Ac-IETD-pNA (caspase-8), and Ac-LEHD-pNA (caspase-9), and incubated for 2 h at 37 °C. Wells containing 90 μl of assay buffer and 10 μl of substrate were used as blank while untreated-cells extract was used as negative control. Absorbance was measured at 405 nm with a Tecan Safire microplate spectrophotometer using Magellan software. Caspase activity was calculated after subtracting the average absorbance of blank wells.

Caspase inhibition assay

To confirm the involvement of caspases in DPT-induced apoptosis, DPT-treated cells viability was assessed after pretreatment of

glioblastoma cells with a broad-spectrum inhibitor of caspases; z-VAD-fmk (Merck Biosciences, Schwalbach, Germany). Briefly, cells were seeded in 96-well plates at appropriate seeding densities. Following 24 h growth, cells were either untreated or pretreated with 100 μM pan-caspase inhibitor (z-VAD-fmk) for 4 h, followed by exposure to DPT (90 nM) for a further 36 h. Cell viability was then measured using a CCK-8 assay.

Mitochondrial membrane potential (JC-1) assay

The loss of mitochondrial membrane potential ($\Delta\Psi m$) is a hallmark for apoptosis [18]. JC-1 (5,5′,6,6′-tetrachloro-1,1′,3,3′-tetraethylbenzimidazolylcarbocyanine iodide) dye was used to monitor mitochondrial membrane potential. Briefly, U-87 MG and SF126 cells were seeded in 6-well plates. After being allowed to adhere, cells were treated with DPT (90 nM) for 12, 24 and 36 h. Following treatment, cells were washed with PBS and incubated with JC-1 reagent in the dark for 30 min at 37 °C in complete medium. Cells were then washed twice with JC-1 staining buffer and 2 ml of medium were added to each well. Thereafter, the cells were analyzed under a fluorescent microscope (Olympus IX71, Tokyo, Japan).

Protein extraction and Western blotting

After DPT exposure, cells were washed with ice-cold PBS and proteins were extracted using the KeyGEN Total Protein Extraction Kit following the manufacturer's instructions. Protein concentrations were determined by the BCA method. Extracts were stored at −80 °C until use.

For Western blot analysis, equal amounts of proteins were electrophoresed on 10% sodium dodecylsulfate polyacrylamide gel electrophoresis (SDS-PAGE) gels and transferred to polyvinylidene difluoride (PVDF) membranes (0.22 μm, Bio-Rad Laboratories, Hercules, CA, USA) by electroblotting. Protein signals on PVDF membranes were assessed with the ChemiDoc XRS imaging densitometer (Bio-Rad), using the Quantity One software program (Bio-Rad Laboratories, CA, USA).

Statistical analysis

Results were expressed as mean ± standard deviation (SD) of separate experiments ($n = 3$) and statistically compared with the control group using Student t-test. A value of $p < 0.05$ was considered to be statistically significant.

Results

DPT induced growth inhibition of human cancer cell lines in vitro

In this study, a panel of human cancer cell lines of different origins was used to evaluate the *in vitro* growth inhibition action of DPT. The results, expressed as the concentration of the compounds required to inhibit cell growth by 50% (IC_{50}), are summarized in Table 1. The *in vitro* screening results showed that DPT possesses a considerable cytotoxic activity since it has inhibited the growth of all tested cancer cell lines with IC_{50} concentrations ranging between 13.95 and 26.72 nM while etoposide was less effective ($IC_{50} \geq 73.57$ nM) (Table 1).

DPT induced morphological changes of U-87 MG and SF126 brain tumor cells

Cells treated with DPT (90 nM) show dramatic changes noted in morphology with nuclear condensation, cells size which became smaller, apparition of rounded cell bodies, loss of adhesion, sporadical distribution, and interrupted cell membranes. Cells detached within 24 h. After 36 h, cells became sparse under field of vision. There was a clear concentration- and time-response tendency. Meanwhile, the untreated tumor cells exhibited typical growth patterns and normal morphology (Fig. 1B). The chromatin condensation, membrane blebbing, and loss of overall cell shape, observed among the two cell lines, indicate the possibility of apoptosis occurrence.

DPT inhibited microtubule assembly

The effect of DPT on glioblastoma cells was compared to that of the reference anti-tubulin compound Paclitaxel which was used as a polymerization positive-control. As shown in Fig. 1C.a, the microtubule network exhibited normal arrangement and organization in untreated cells. Twelve hours after DPT-treatment (30 nM), dramatic changes in microtubule assembly were observed. Indeed, DPT significantly induced cellular microtubule depolymerization with short microtubules in the cytoplasm. Cells have lost their normal cellular shape and became round (Fig. 1C.b). Nuclear fragmentation and chromatin condensation, known as the classic characteristics of apoptosis, were clearly observed after 36 h (Fig. 1C.c). In contrast, treatment with a microtubule stabilizer, paclitaxel, dramatically promoted tubulin polymerization with an increase in the density of cellular microtubules compared to the control cells (Fig. 1C.d and e).

Alteration of the cell cycle

Flow cytometric analysis showed that U-87 MG and SF126 cells treated with DPT were dose- and time-dependently arrested in the G2/M phase of the cell cycle. (Fig. 2A–D). Furthermore, a typical apoptosis-related hypodiploid DNA content peak (sub-G1) was detected in the DPT-treated cells after 24 h. This peak markedly increased after 36 h; about 31.88% and 37.80% of SF126 and U-87 MG cells, respectively, were in the apoptotic phase (Fig. 2C and D).

Table 1
Antiproliferative activity data of DPT against different human cancer cell lines.

Cell lines	Origin	DPT IC_{50} (nM)[a]	VP-16[b] IC_{50} (nM)[a]	VP-16 IC_{50}/DPT IC_{50}
SF126	Glioblastoma	13.95 ± 0.19	701.95 ± 53.39	50.32
U-87 MG	Glioblastoma	15.06 ± 0.46	588.31 ± 48.64	39.06
SGC-7901	Gastric carcinoma	19.72 ± 0.46	5465.59 ± 2125.91	277.16
BGC-823	Gastric carcinoma	26.72 ± 2.39	9481.53 ± 1664.08	354.85
HO-8910	Ovarian carcinoma	21.57 ± 0.81	3327.90 ± 264.32	154.28
SK-0V-3	Ovarian carcinoma	25.15 ± 0.04	2161.79 ± 437.20	85.96
HT-29	Colon carcinoma	18.72 ± 0.33	16,162.57 ± 5480.62	863.39
MDA-MB-231	Breast carcinoma	21.80 ± 1.53	434.72 ± 34.20	19.94
JeG-3	Choriocarcinoma	25.25 ± 0.62	73.57 ± 60.34	2.91

[a] Values, expressed as IC_{50} (50% growth inhibition), are given in nanomole (nM) and are mean ± SD of three independent experiments.
[b] VP-16: Etoposide.

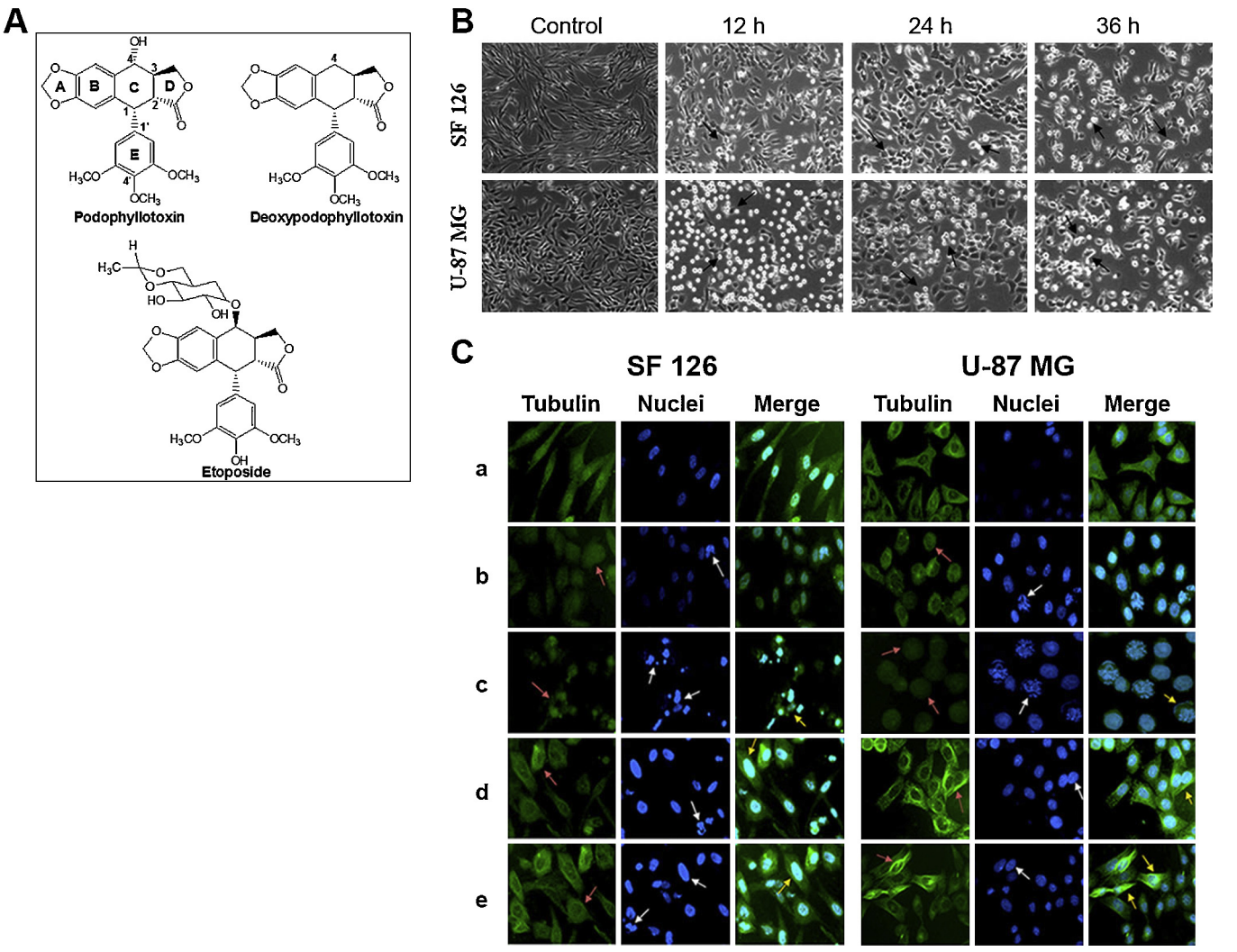

Fig. 1. DPT induces microtubule disassembly and DNA fragmentation. (A) Chemical structures of podophyllotoxin, deoxypodophyllotoxin (DPT) and etoposide. (B) Following DPT-treatment for different lengths of time as indicated, U-87 MG and SF126 cells were observed under an inverted light microscope. Magnification: ×10. (C) Cells grown on coverslips were treated with DPT (30 nM) and Paclitaxel for 12 and 36 h, fixed and immunostained. Microtubules (green) were stained by incubation with a monoclonal anti-α-tubulin antibody for 1 h and then with Alexa-Fluor 488-conjugated secondary antibody. Chromosomal DNA (blue) was counterstained with Hoechst 33258 dye. Magnification: ×20. (a) Control, (b) DPT-12 h, (c) DPT-36 h, (d) paclitaxel-12 h, (e) paclitaxel-36 h. (For interpretation of the references to color in this figure legend, the reader is referred to the web version of this article.)

DPT induced changes in the expression of G2/M regulatory proteins

Western blot analysis was performed to examine the expression of the main cell cycle regulatory proteins at the G2/M boundary, including p21, cyclin B1, Cdc2, and Cdc25C. The results showed that DPT up-regulated p21 protein levels in both glioblastoma treated-cell lines in a time-dependent manner (Fig. 2E and F). Meanwhile, the levels of cyclin B1, Cdc2, and Cdc25C proteins started to decrease after 24 h and almost disappeared after 36 h in U-87 MG cells (Fig. 2E and F). On the other hand, DPT up-regulated cyclin B1 protein after 12 h, and had no effect on the expression of Cdc2 in SF126 cells. The Cdc25's mitotic migration band was detected in SF126 cells 12 h after DPT-treatment (Fig. 2E and F).

DPT induced apoptosis through the activation of caspase-8 and caspase-9

To further investigate the action of DPT on U-87 MG and SF126 brain tumor cells, Annexin V/propidium iodide (PI) double staining assay was performed to check whether DPT could induce apoptosis. Early apoptosis is detected by positive staining for Annexin V-FITC (Annexin V+/PI−) while later stage apoptosis indicating a complete loss of membrane integrity and DNA damage shows positive staining for both Annexin V and PI (Annexin V+/PI+) [19,20].

Quantitative analysis using Annexin V/PI binding assay after 36 h of DPT-treatment (30, 60 and 90 nM) resulted in 50.53%, 70.01% and 73.09% (U-87 MG), and 41.74%, 44.44%, and 49.46% (SF126) Annexin-positive apoptotic cells compared with 1.72% (U-87 MG), and 3.36% (SF126) spontaneous apoptosis in negative control (Fig. 3A). Detailed results have been summarized in Table 2.

To examine whether DPT-induced U-87 MG and SF126 cell death is dependent upon caspases, we evaluated its effect for the activation of the main caspases-3, -8, and -9 [21].

We firstly examined the effect of DPT on caspase-3, a downstream executioner of caspase-8 and -9 [22]. Compared to the control group, incubation of U-87 MG and SF126 cells with DPT resulted in the activation of caspase-3 in a dose- and time-dependent manner (Fig. 3B). The activation of caspase 3 was also confirmed by the Western blot results *via* examining PARP which is an endogenous substrate for caspase 3 and an early marker of

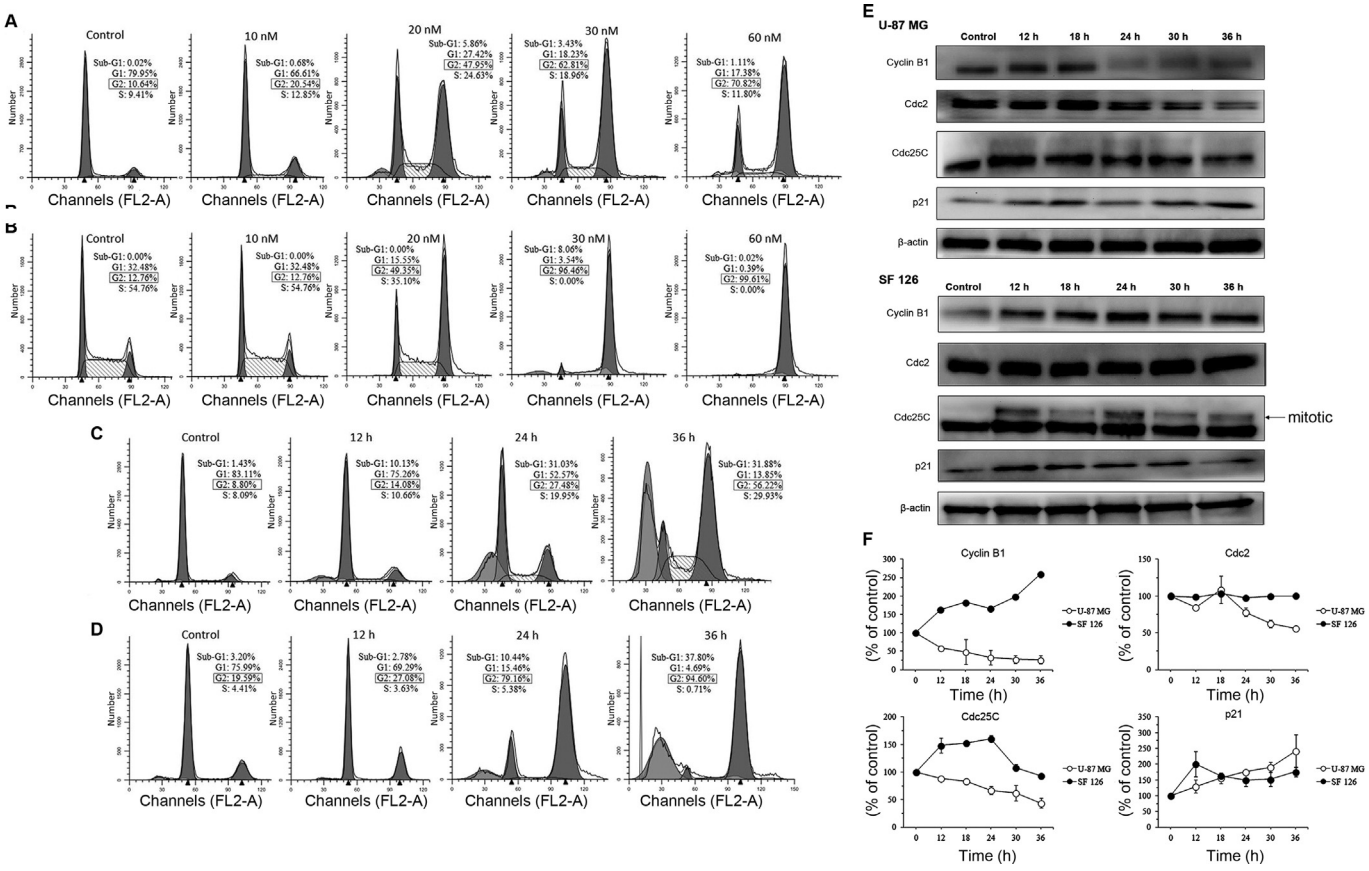

Fig. 2. DPT induces G2/M phase arrest in U-87 MG and SF126 cell lines. (A, C) SF126; (B, D) U-87 MG: Following DPT treatment, cells were analyzed for PI-stained DNA content by flow cytometry. (E) Cells were treated with DPT for various periods of time as indicated. At each time point, expressions of cyclin B1, Cdc2, Cdc25C, and p21 proteins were analyzed by Western blotting. (F) Relative band intensities (normalized to β-actin) shown in E were measured using Quantity One software. Values are plotted as the mean ± SD ($n = 3$).

apoptosis. Western blot analysis revealed that DPT induced the cleavage of PARP (116 kDa) into its smaller fragment (85 kDa) (Fig. 4C and D).

To understand the mechanism by which caspase-3 was activated by DPT, we further investigated its effect on the activity of caspase-8 and -9, upstream activators of caspase-3. Our results demonstrate that DPT induces the activation of these caspases in both glioblastoma cell lines.

DPT-treatment dissipated the mitochondrial membrane potential ($\Delta\Psi m$) and reduced the expression of anti-apoptotic molecules Bcl-2 and Bcl-xL

To further characterize DPT-induced apoptosis in U-87 MG and SF126 glioblastoma cells, we examined the change of the mitochondrial membrane potential using JC-1 staining assay [23]. This cationic mitochondrial vital dye exhibits potential-dependent accumulation in mitochondria, as represented by a shift of fluorescence emission from orange-red in normal polarized mitochondria to green in abnormal depolarized ones (apoptotic cells) [24]. As shown in Fig. 4A, DPT induced a dramatic change of JC-1 color with cells emitting orange-red fluorescence in non-treated control samples whereas DPT-treated cells emitted green fluorescence suggesting that DPT induced a severe damage to mitochondria. In order to quantify the mitochondrial depolarization induced by DPT, we used FACS analysis with JC-1 staining to examine the change in $\Delta\Psi$m. Data shown in Fig. 4B indicate a significant increase ($p < 0.05$) in the percentage of cells with depolarized mitochondria upon DPT-treatment. These results are consistent with the fluorescent microscopy observations. Furthermore, analysis of the cellular levels of Bcl-2 and Bcl-xL proteins showed that DPT resulted in a down-regulation of these anti-apoptotic molecules (Fig. 4C and D).

Discussion

The microtubules are an attractive target for many chemotherapeutic agents [25–27]. In this paper, we evaluated the *in vitro* antiproliferative activity of a plant-derived semi-synthetic compound, DPT. Its predicted effectiveness is based on structural analogy with podophyllotoxin, a potent antitumor agent known to depolymerize microtubules. The *in vitro* cytotoxicity study revealed that DPT has a potent growth-inhibitory effect against brain, colon, gastric, breast, and ovarian cancer cells. Indeed, our results showed that DPT possesses broad-spectrum ability at the nanomolar range to inhibit the growth of a wide panel of human cancer cell lines. It is noteworthy that its action was more potent than that of the well-known cytostatic agent; etoposide.

To gain further insight into the mode of action, DPT was assayed for its effect on glioblastoma U-87 MG and SF126 cell lines. Based on flow cytometric analysis, DPT has been shown to induce G2/M phase arrest in a time- and dose-dependent manner. The cell cycle is a highly regulated process involving cyclins and cyclin-dependent kinases such as cyclin B1 and Cdc2 which play a key role in regulating the phosphorylation or dephosphorylation of different proteins [28]. Indeed, the Cdc2/cyclin B complex is one

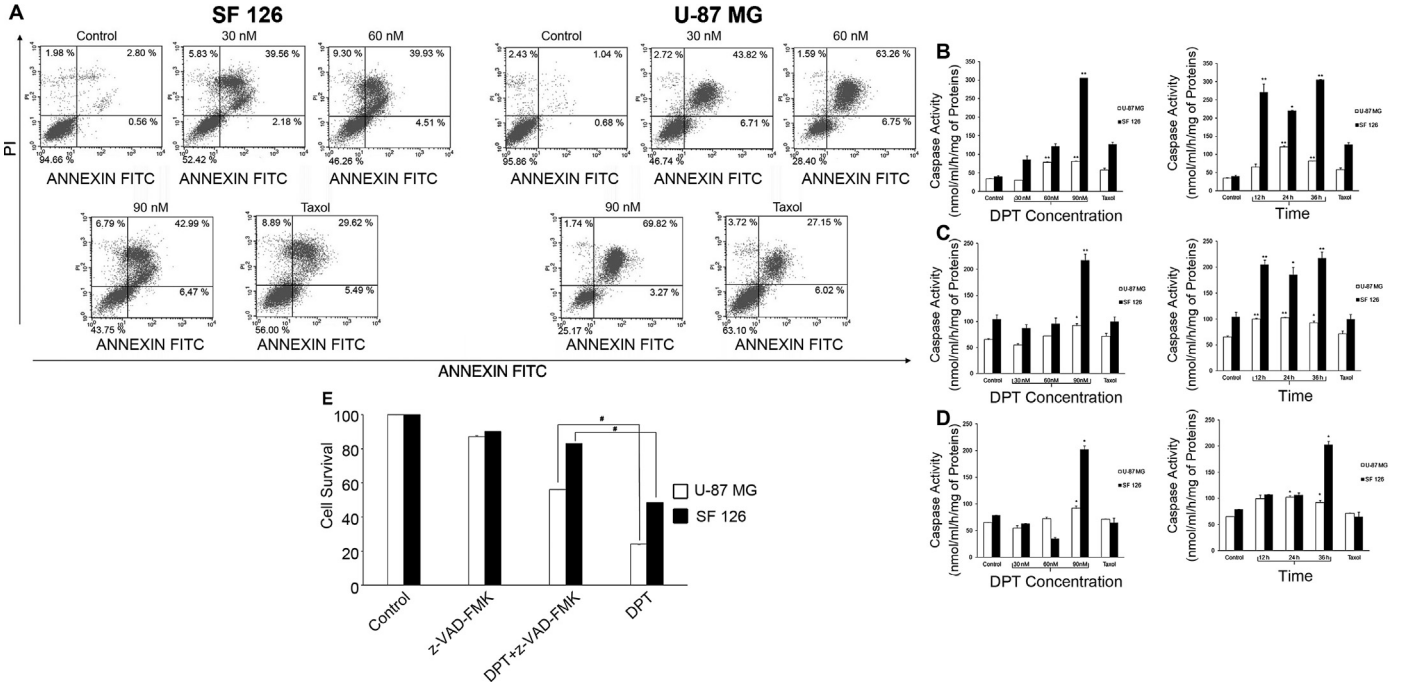

Fig. 3. DPT induces apoptosis *via* caspase-8 and -9 dependent pathways. (A) After incubation for 36 h with DPT and Paclitaxel (positive control), cells were harvested, washed with PBS, stained with Annexin V-FITC and PI, and analyzed by flow cytometry. (B) Caspase-3; (C) caspase-8; (D) caspase-9: After treatment, cells were collected and lysed. The activities of caspase-3, -8 and -9 were detected by their enzymatic cleavage of specific colorimetric substrates: DEVD-pNA, IETD-pNA and LEHD-pNA, respectively. (E) Cells were either untreated or pretreated with 100 μM of pan-caspase inhibitor z-VAD-fmk for 4 h, then treated with DPT for a further 36 h. The cell survival was determined by CCK-8 assay. Each bar represents the mean ± SD of data from three independent experiments. * $p < 0.05$, ** $p < 0.01$ *versus* control. # $p < 0.05$ compared to DPT alone within the treated groups.

of the major regulators governing the G2 to M progression or apoptosis [29]. Cells with a suppressed cyclin B1/Cdc2 activity would be arrested in the G2 phase, whereas cells with an elevated cyclin B1/Cdc2 activity would tend to be favored to enter and proceed through mitosis [30]. Induction of mitosis and meiosis (M phase) in the eukaryotic cell cycle requires activation of the Cdc2/cyclin B complex by the protein phosphatase Cdc25 [31]. In addition to cyclin B1, Cdc2, and Cdc25C; p21 protein functions as a regulator of cell cycle progression. It has been previously reported that p21 induces cell cycle arrest [32] and its activation has been shown to participate in G0/G1 as well as G2/M phase arrest of cell cycle [33,34]. DPT-treated U-87 MG and SF126 cells showed an increase expression of p21 protein. Since FACS analysis could not distinguish between cell populations in G2 and M phase, modifications in the expression of G2/M cell cycle regulatory proteins induced by DPT were analyzed using Western blotting. Results revealed that U-87 MG glioblastoma cells showed G2 phase arrest after DPT-treatment. In this cell line, DPT reduced the cellular levels of both Cdc2 and cyclin B1 proteins. In addition, the decreased level of Cdc25C by DPT may inhibit the action of Cdc2. In contrast, DPT failed to down-regulate Cdc2 and rather up-regulated cyclin B1 in SF126 glioblastoma cells which suggest that DPT induced M phase arrest in these cells. Therefore, a potential mechanism for DPT-induced G2 arrest in U-87 MG glioblastoma cells was through a decrease of the total protein levels of Cdc2, cyclin B1, and Cdc25C. The decrease of the expression of these proteins by DPT inhibited these glioblastoma cells from entering M phase. On the other hand, DPT-induced M arrest in SF126 glioblastoma cells might be due to up-regulated expression of cyclin B1.

Microtubules—key components of the cytoskeleton—have been shown to play a crucial role in the development and maintenance of cell shape, transport of vesicles, mitochondria and other components throughout cells, in cell division and cell signaling [26]. Since DPT arrested glioblastoma cells at G2/M phase of the cell cycle, we wondered whether our compound interferes with microtubule assembly. Data from immunofluorescence microscopy clearly demonstrate that DPT strongly depolymerizes microtubules.

It is widely accepted that microtubule-interfering agents produce apoptosis by causing cell cycle arrest [35]. The various morphological and molecular events that may occur during apoptosis have already been identified [36]. In addition to the effect of DPT on the cell cycle, we found that it also provokes

Table 2
Annexin V/PI assay data after 36 h of DPT-treatment.

Cell lines		Control	Paclitaxel[a]	DPT		
				30 nM	60 nM	90 nM
SF126	Live cells	94.41 ± 0.35	44.24 ± 16.64	49.86 ± 3.62	41.14 ± 7.25	38.28 ± 7.74
	Early apoptotic cells	0.51 ± 0.08	5.65 ± 0.23	2.1 ± 0.12	3.35 ± 1.64	7.18 ± 1.00
	Late apoptotic cells	1.72 ± 1.53	33.52 ± 5.52	34.21 ± 7.57	43.47 ± 5.01	44.38 ± 1.96
U-87 MG	Live cells	94.58 ± 1.81	63.06 ± 0.06	48.63 ± 2.67	29.79 ± 1.97	28.06 ± 4.09
	Early apoptotic cells	1.06 ± 0.54	3.19 ± 4.01	3.41 ± 4.67	3.76 ± 4.23	2.03 ± 1.75
	Late apoptotic cells	1.49 ± 0.63	24.21 ± 4.16	39.51 ± 6.10	61.00 ± 3.20	64.73 ± 7.21

Results are given in % and are mean ± SD of three independent experiments.
[a] Paclitaxel (90 nM) was used as a positive control.

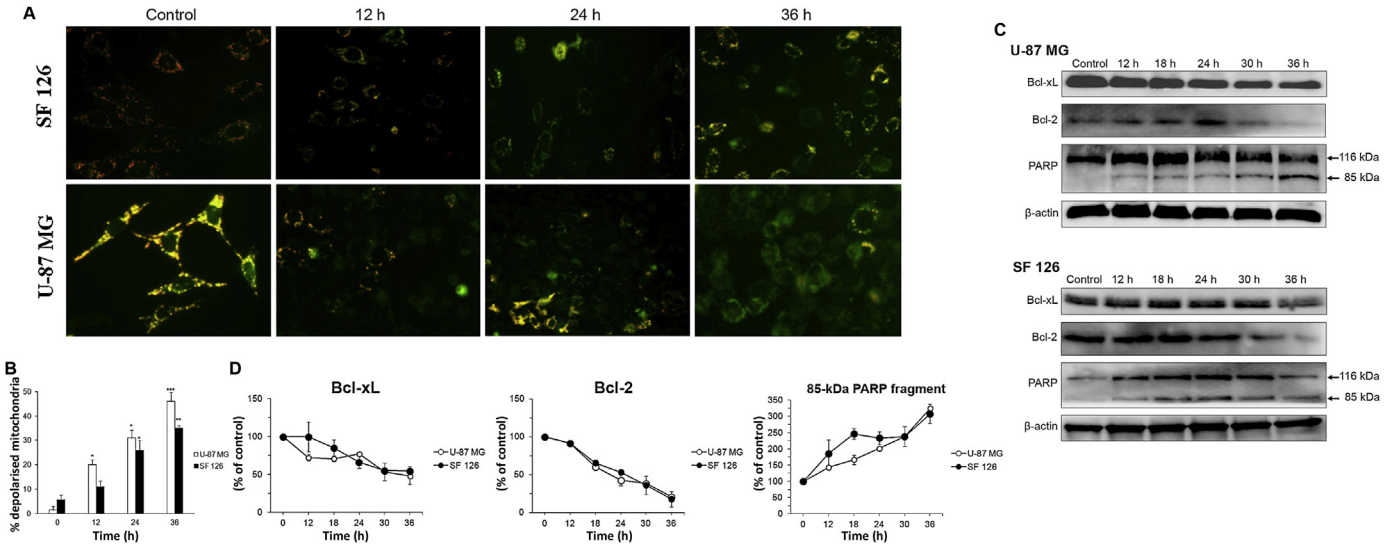

Fig. 4. DPT-treatment leads to mitochondrial membrane depolarization, down-regulation of anti-apoptotic proteins Bcl-2 and Bcl-xL and cleavage of PARP. (A) Cells were seeded in 6-well plate for 24 h. Following treatment with DPT, cells were washed with PBS and incubated with 1 ml/well of JC-1 dye for 30 min at 37 °C. Pictures were taken under a fluorescent microscope. Magnification: ×20. (B) Percentages of glioblastoma cells with depolarised mitochondria determined by flow cytometry. (C) Cells were treated with DPT for the indicated time course and the whole cell lysates were analyzed for the anti-apoptotic proteins Bcl-2 and Bcl-xL and for the cleaved form of PARP by Western blotting. (D) Relative band intensities (normalized to β-actin) shown in B were measured using Quantity One software. Values are plotted as the mean ± SD ($n = 3$). * $p < 0.05$, ** $p < 0.01$, *** $p < 0.001$ *versus* control. (For interpretation of the references to color in the text, the reader is referred to the web version of this article.)

apoptosis, as indicated by an increase in the sub-G1 population, DNA fragmentation and Annexin V positivity (Figs. 1C, 2C, D and 3A; Table 2). Our results from caspase activity assay and Western blot analysis also showed that DPT promotes the activation of caspase-3 (Fig. 3B) which is accompanied by the cleavage of its well-known substrate PARP into a 85 kDa C-terminal fragment (Fig. 4C), indicating that the mechanism of DPT-induced apoptosis involves a caspase-mediated pathway [37]. This was confirmed by the fact that inhibition of caspases activity by a general caspase inhibitor (z-VAD-fmk) prevented DPT-induced growth inhibition of glioblastoma cells. We also observed the induction of caspase-8 and -9 after DPT exposure in a dose- and time-dependent manner (Fig. 3C and D). Furthermore, we detected a loss of mitochondrial membrane potential (Fig. 4A) and a down-regulation of the cellular levels of anti-apoptotic proteins Bcl-2 and Bcl-xL (Fig. 4C and D). Therefore, DPT triggers cell death *via* both the extrinsic and intrinsic apoptotic pathways.

In summary, our study demonstrates, for the first time, that the antitumor effect of DPT is time-, dose, and cell line-dependent. Hence from these data it can be concluded that DPT has not only shown a significant *in vitro* cytotoxic activity but has provided an insight for future direction in the development of such molecules.

Funding

This study was partially supported by the 111 Project (111-2-07), 2011 Program for Excellent Scientific and Technological Innovation Team of Jiangsu Higher Education and National 12th Five-year Plan "Major Scientific and Technological Special Project for Significant New Drugs Creation" project (No. 2012ZX09504001-001).

Conflicts of interest

All authors declare no conflicts of interest.

References

[1] Kohler BA, Ward E, McCarthy BJ, Schymura MJ, Ries LA, Eheman C, et al. Annual report to the nation on the status of cancer, 1975–2007, featuring tumors of the brain and other nervous system. J Natl Cancer Inst 2011;103:714–36.
[2] Zülch KJ. Brain tumors; their biology and pathology. Berlin: Springer-Verlag; 1986.
[3] CBTRUS Statistical Report. Statistical report: primary brain tumors in the United States, 2000–2004. Chicago: Central Brain Tumor Registry of the United States; 2008 Available from:www.cbtrus.org.
[4] Fomchenko EI, Holland EC. Mouse models of brain tumors and their applications in preclinical trials. Clin Cancer Res 2006;12:5288–97.
[5] Affronti ML, Heery CR, Herndon 2nd JE, Rich JN, Reardon DA, Desjardins A, et al. Overall survival of newly diagnosed glioblastoma patients receiving carmustine wafers followed by radiation and concurrent temozolomide plus rotational multiagent chemotherapy. Cancer 2009;115:3501–11.
[6] Dall'Acqua S, Giorgetti M, Cervellati R, Innocenti G. Deoxypodophyllotoxin content and antioxidant activity of aerial parts of *Anthriscus sylvestris* Hoffm. Z Naturforsch C 2006;61:658–62.
[7] van Maanen JM, Retel J, de Vries J, Pinedo HM. Mechanism of action of antitumor drug etoposide: a review. J Natl Cancer Inst 1988;80:1526–33.
[8] Shah JC, Chen JR, Chow D. Preformulation study of etoposide: identification of physicochemical characteristics responsible for the low and erratic oral bioavailability of etoposide. Pharm Res 1989;6:408–12.
[9] Imbert TF. Discovery of podophyllotoxins. Biochimie 1998;80:207–22.
[10] Zhou J, Xie G, Yan X. Encyclopedia of traditional Chinese medicines. Vol. 5 – molecular structures, pharmacological activities, natural sources and applications. New York: Springer; 2011.
[11] Jiangsu New Medical College. Dictionary of Chinese traditional medicine. Shanghai: Shanghai Science and Technology Press; 1986.
[12] Jiang RW, Zhou JR, Hon PM, Li SL, Zhou Y, Li LL, et al. Lignans from *Dysosma versipellis* with inhibitory effects on prostate cancer cell lines. J Nat Prod 2007;70:283–6.
[13] Yu PZ, Wang LP, Chen ZN. A new podophyllotoxin-type lignan from *Dysosma versipellis* var. *tomentosa*. J Nat Prod 1991;54:1422–4.
[14] Shang MY, Xu LS, Li P, Xu GJ, Wang YX, Cai SQ. Study on pharmacodynamics of Chinese herbal drug Guijiu and its lignan. Chin Tradit Herb Drugs 2002;33(8):722–4.
[15] Wigley DB. Structure and mechanism of DNA topoisomerases. Annu Rev Biophys Biomol Struct 1995;24:185–208.
[16] Rassmann I, Thodtmann R, Mross M, Huttmann A, Berdel WE, Manegold C, et al. Phase I clinical and pharmacokinetic trial of the podophyllotoxin derivative NK611 administered as intravenous short infusion. Invest New Drugs 1998;16:319–24.
[17] Ayres DC, Loike JD. Lignans: chemical, biological and clinical properties. In: Chemistry and pharmacology of natural products. Cambridge, UK: Cambridge University Press; 1990.
[18] Ankarcrona M, Dypbukt JM, Bonfoco E, Zhivotovsky B, Orrenius S, Lipton SA, et al. Glutamate-induced neuronal death: a succession of necrosis or apoptosis depending on mitochondrial function. Neuron 1995;15:961–73.
[19] Vermes I, Haanen C, Steffens-Nakken H, Reutelingsperger C. A novel assay for apoptosis. Flow cytometric detection of phosphatidylserine expression on

early apoptotic cells using fluorescein labelled Annexin V. J Immunol Methods 1995;184:39–51.
[20] Lee MK, Lim SJ, Kim CK. Preparation, characterization and *in vitro* cytotoxicity of paclitaxel-loaded sterically stabilized solid lipid nanoparticles. Biomaterials 2007;28:2137–46.
[21] Thornberry NA. Interleukin-1 beta converting enzyme. Methods Enzymol 1994;244:615–31.
[22] Al-Rubeai M, Fussenegger M. Apoptosis. Kluwer Academic Publishers; 2004.
[23] Salvioli S, Ardizzoni A, Franceschi C, Cossarizza A. JC-1, but not DiOC6(3) or rhodamine 123, is a reliable fluorescent probe to assess delta psi changes in intact cells: implications for studies on mitochondrial functionality during apoptosis. FEBS Lett 1997;411:77–82.
[24] Cossarizza A, Baccarani-Contri M, Kalashnikova G, Franceschi C. A new method for the cytofluorimetric analysis of mitochondrial membrane potential using the J-aggregate forming lipophilic cation 5,5′,6,6′-tetrachloro-1,1′,3,3′-tetraethylbenzimidazolcarbocyanine iodide (JC-1). Biochem Biophys Res Commun 1993;197:40–5.
[25] Islam MN, Iskander MN. Microtubulin binding sites as target for developing anticancer agents. Mini Rev Med Chem 2004;4:1077–104.
[26] Jordan MA, Wilson L. Microtubules as a target for anticancer drugs. Nat Rev Cancer 2004;4:253–65.
[27] Teicher BA. Newer cytotoxic agents: attacking cancer broadly. Clin Cancer Res 2008;14:1610–7.
[28] Nurse P. Universal control mechanism regulating onset of M-phase. Nature 1990;344:503–8.
[29] Castedo M, Perfettini JL, Roumier T, Kroemer G. Cyclin-dependent kinase-1: linking apoptosis to cell cycle and mitotic catastrophe. Cell Death Differ 2002;9:1287–93.
[30] Ohi R, Gould KL. Regulating the onset of mitosis. Curr Opin Cell Biol 1999;11:267–73.
[31] Morgan DO. Cyclin-dependent kinases: engines, clocks, and microprocessors. Annu Rev Cell Dev Biol 1997;l 13:261–91.
[32] Gartel AL, Tyner AL. The role of the cyclin-dependent kinase inhibitor p21 in apoptosis. Mol Cancer Ther 2002;1:639–49.
[33] Brehm A, Miska EA, McCance DJ, Reid JL, Bannister AJ, Kouzarides T. Retinoblastoma protein recruits histone deacetylase to repress transcription. Nature 1998;391:597–601.
[34] Flatt PM, Tang LJ, Scatena CD, Szak ST, Pietenpol JA. p53 regulation of G(2) checkpoint is retinoblastoma protein dependent. Mol Cell Biol 2000;20:4210–23.
[35] Mollinedo F, Gajate C. Microtubules, microtubule-interfering agents and apoptosis. Apoptosis 2003;8:413–50.
[36] Hacker G. The morphology of apoptosis. Cell Tissue Res 2000;301:5–17.
[37] Nicholson DW, Ali A, Thornberry NA, Vaillancourt JP, Ding CK, Gallant M, et al. Identification and inhibition of the ICE/CED-3 protease necessary for mammalian apoptosis. Nature 1995;376:37–43.